Dynamic modelling and control of a luxury arts and crafts product

Mathieu Porez, Victorien Ferr É

Dynamic modelling and control of a luxury arts and crafts product.

Mathieu POREZ * **Victorien FERRÉ** **

* *LS2N - IMT Atlantique - La Chantrerie, 4, rue Alfred Kastler, B.P. 20722, 44307 Nantes, Cedex 3, France*
** *PA.COTTE - 2, rue Adrienne Bolland, 44980 Sainte Luce sur Loire, France*

Abstract: This paper deals with the modelling and control of a hinge integrated in a luxury product. In this context, following the works of Boyer and Belkhiri (2014) on modelling of multibody systems, an application of Newton-euler algorithms and space reduction processes to a mechanism with closed loops is proposed. Especially, a focus to a special linkage namely "cam and follower" mechanism which is a closed loop whose the contact point moves along a curve carried by the bodies, is done. Regarding the integration, a dynamic controller, i.e a computed torque algorithm, has been implemented in a mock-up of the opening system under consideration. The solution allowed us to control, with the expected performance, the opening and closing of a lid.

Keywords: Multibody system, dynamic modelling, control, cam and follower mechanism.

1. INTRODUCTION

Over the centuries, the arts and crafts has focused to the traditional handwork such as the furniture, ceramics, goldsmiths, jewelry, textiles and the watchmaking. Under the impulse of the first and second industrial revolutions, even if arts and industry are conceptually opposed to each other, the new techniques & methods allowed craftsmen to work with more precision and delicacy, as well as to produce more complex, qualitative and reliable works. For example, at that time, the advance in micro-mechanics allowed the miniaturization and complexity of the watch kinematics. Even today, in the market of industrial arts, important investments and researches are done to improve techniques & methods, like those in the fields of the machining and polishing of high value-added materials like titanium, which find today in many luxury product. With the advent of the Internet, for the past 10 years, the industry has been making its forth revolution, and is opening up to the Cloud technologies as the Internet of Things, the robotics, the decision making AI, and so on ... As far as the arts and crafts industry is concerned, it is not left out. In particular, surfing on this trend, the international group PA.COTTE SA has launched an innovative initiative which gives pride of place to robotics and IoT in a luxury craft product. Indeed, dozen of mechanisms fully controlled in their automatic movements, made of high value-added materials, matched with precious stones, integrated in an everyday Cloud connected product, it is the magical wedding between high technologies and craftsmanship in progress in PA.COTTE. To succeed in this challenge, i.e to control complex mechanisms according to the standards of luxury and the expectations of the buyers, the theory of robotics modelling, in particular this of multibody system is intensively used. In the continuity of the works of Boyer and Belkhiri (2014); Boyer and Porez (2015); Boyer et al. (2018) dedicated to the dynamic modelling of a mobile multibody system under non-holonomic constraints, the issue addressed in the article concerns with the modelling and control of an opening mechanism in a PA.COTTE's product. In addition to closed loops, its main characteristic is to integrate a "cam and follower" mechanism for which, contrary to a classical closed loop, the internal contact point slides along the bodies. As the reader will see, from a mathematical description of the curve defining the cam, it is possible to track the contact point in its motion, to write a holonomic constrain and finally, to reduce and to solve the forward dynamic problem of the mechanism. Let us note that such a strategy has been successfully used in Fisette and Samin (1994); Fisette et al. (2000) for the design and the optimization of cam and follower mechanisms. Here, we propose to exploit the methodology and the fast algorithm from Boyer and Belkhiri (2014) to this type of mechanism and to address its dynamic control. For this purpose, the article is structured as follows. After the introduction of notations, see Sec. 2, the dynamic modelling of a multibody system is introduced in Sec. 3. Then, these models are exploited in Sec. 4, in the context of a hinge and a cam and follower mechanism. Their dynamic control is discussed in Sec. 5. Lastly, the article ends with some numerical and experimental illustrations, see Sec. 6, as well as a conclusion, see Sec. 7.

2. PARAMETRISATION AND NOTATIONS.

As represented in Fig. 1, the multibody system under consideration has a tree-like structure with closed loops composed of a sequence of $n+1$ rigid bodies interconnected

[1] The authors would like to thank T. CARRÉ, J.-F. CHEVALIER, P. HUGUES and F. MAHOT for their technical supports, and especially P.-A. COTTE, the chairman of PA.COTTE SA, for his technical and financial supports.

by n revolute or prismatic joints with one degree of freedom each. The bodies are numbered from the base $\mathcal{B}_0$ (bounded to the ground) to the tips of the branches $\mathcal{B}_n$ in ascending order. We denote by j and $i = a(j)$, the indices of the current body and its antecedent respectively. We attach to each body $\mathcal{B}_j$ an orthonormal frame $\mathcal{F}_j = (O_j, s_j, n_j, a_j)$. Depending on the studied system, the axis of joints can be arbitrary supported by any basis vector. To specify the orientation and type of joint, we define the vector $A_j \in se(3)$ whose, in the prismatic joint case, its first three components will be equal to the unit vector of $\mathcal{F}_j$ supporting the joint whereas, in the case of a revolute one, the previous equality will be done on the three last components of A_j. At any time t, the configuration is defined by the vector of joint positions $r = (r_1, ..., r_n)^T \in \mathbb{R}^n$ defining the relative angles or distances around or along the joint axis between the bodies respectively. As far as the closed loops are concerned, they are modelled as a set of holonomic constraints. In practice, these constraints are deduced by forcing, at the point of contact between concerned bodies, the relative velocity to be zero. If we define by p the number of independent constraints, the mobility of the system will be equal to $n - p$ degrees of freedom. Finally, we will use the Newton-Euler formalism in robotics as introduced in Khalil and Dombre (2002) to model the considered systems. In fact, for the past years, the Newton-Euler model has been extensively exploited to generate efficient and simple algorithm to solve the inverse, forward or hybrid dynamic problems of multibody systems or mobile multibody systems like Khalil et al. (2007); Featherstone (2008); Porez et al. (2014) and so on. Lastly, throughout this article, we will use the following notational conventions. For any physical variable modelled by a tensor, the lower right subscript will represent the index of the body (to which it is related) while the upper left superscript will denote the index of the reference frame, which is also the projection frame. When the tensor relative to a body is expressed in its frame, the superscript is omitted.

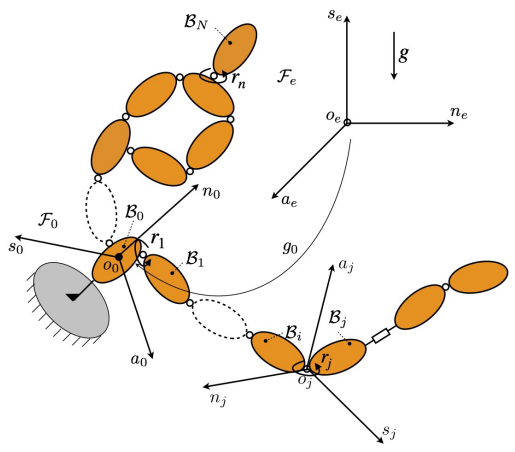

Fig. 1. Schematic view of a multibody system.

3. REDUCED DYNAMICS OF A MULTIBODY SYSTEM.

In accordance with the definitions of Sec. 2, we address the following forward dynamic problem: knowing at each time t, the state of the multibody system $x^T = (\dot{r}^T, r^T)$, and the vector of control torques applied on the joints $\Gamma \in \mathbb{R}^n$; it consists in calculating the joint accelerations $\ddot{r}$ and the wrench of the reaction forces f_0 applied by $\mathcal{B}_0$ on the ground. From Boyer and Belkhiri (2014), the forward dynamic equations can be written in the following assembled Lagrangian form:

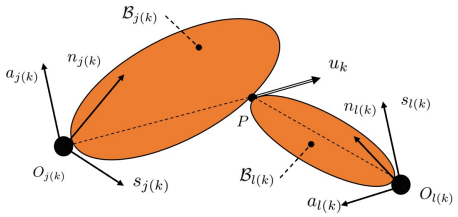

Fig. 2. The k^{th} constraint involving the bodies $\mathcal{B}_{j(k)}$ and $\mathcal{B}_{l(k)}$.

$$\begin{cases} m^+(r)\ddot{r} = -Q^+(r,\dot{r}) + \Gamma + B^T(r)\lambda \\ f_0 = M_0^{+T}(r)\ddot{r} + F_0^+(r,\dot{r}) \end{cases}. \tag{1}$$

In (1), $m^+ \in \mathbb{R}^{p\times p}$ is the internal inertia matrix of the multibody system, $M_0^+ \in se(3)^* \otimes \mathbb{R}^p$ is an inertia coupling matrix between the internal and external dynamics, $Q^+ \in \mathbb{R}^p$ and $F_0^+ \in se(3)^*$ are the vectors of the internal and external forces respectively, and finally $\lambda \in \mathbb{R}^p$ is the vector of Lagrange multipliers which are the reaction forces between bodies involving in the closed loops which are modelled by the p independent holonomic constraints of the following general form: $0_p = B(r)\dot{r}$, where $B \in \mathbb{R}^{p\times n}$ is a matrix deduced from the zero relative speed conditions imposed on the bodies at the contact points closing the loops. As illustrated in Fig. 2, the k^{th} constraint involving the bodies $\mathcal{B}_{j(k)}$ and $\mathcal{B}_{l(k)}$ is:

$$\underbrace{u_k^T \left(J_{S_{j(k)}} - {}^{j(k)}J_{S_{l(k)}} \right)}_{B\delta_k} \dot{r} = 0,$$

where $S_{j(k)}$ and $S_{l(k)}$ are the coordinates of the contact point S according to $\mathcal{F}_{j(k)}$ and $\mathcal{F}_{l(k)}$ respectively, u_k is the unit vector along the constraint is applied while $J_{S_{j(k)}}$ and $J_{S_{l(k)}}$ are Jacobian matrices calculated at S, giving the twists in P in function of $\dot{r}$, i.e:

$$J_{S_{j(k)}} = \begin{pmatrix} 1_3 & {}^j\hat{O}S_{j(k)}^T \\ 0_3 & 1_3 \end{pmatrix} J_{j(k)}, \tag{2}$$

where the Jacobian matrix $J_j \in se(3) \otimes \mathbb{R}^n$ is defined by the recursive equation:

$$J_j = Ad_{j}{}_{g_i} J_i + A_j \delta_j^T \text{ with, } J_0 = 0_{6\times n}. \tag{3}$$

In (3), δ_j is a unit vector whose the jth component is the only one non-zero value while $Ad_{j}{}_{g_i}$ is the adjoint map operator which carries a element of $se(3)$ (like a twist) from $\mathcal{F}_i$ to $\mathcal{F}_j$ (Murray et al. (1994)):

$$Ad_{j}{}_{g_i} = \begin{pmatrix} {}^jR_i & {}^jR_i{}^i\hat{P}_j^T \\ 0_{3\times 3} & {}^jR_i \end{pmatrix}, \tag{4}$$

with ${}^iR_j$ and ${}^iP_j$ the orientation matrix and the position vector of $\mathcal{F}_j$ with respect to $\mathcal{F}_i$. Let us note that in (2) and (4), the 'hat' notation is (3×3) asymmetric tensor associated to (3×1) mentioned vector. For any vectors U and V of $\mathbb{R}^3$, $\hat{U}$ is defined such that $\hat{U}V = U \times V$.

Once the matrix B is known, the dynamics of the system can be reduced by projecting (1) into the kernel of admissible speed subspace $H = \ker(B)$. In practice, this reduction consists, in first step, in reducing the kinematics as follows:

$$\dot{r} = H(r)\dot{r}_r, \text{ and } \ddot{r} = H(r)\ddot{r}_r + \dot{H}(r,\dot{r})\dot{r}_r, \tag{5}$$

where $\dot{r}_r$ is the reduced speeds of joints. In a second step, by introducing (5) into (1), and since $H^T B^T = 0$, we obtain the reduced dynamics (forward form):

$$m_r^+(r)\ddot{r}_r = -Q_r^+(r,\dot{r}) + \tau. \tag{6}$$

In (6), we have introduced the following reduced matrices:

$$m_r^+ = H^T m^+ H, \tag{7}$$

$$Q_r^+ = H^T\left(Q^+ + m^+\dot{H}\dot{r}_r\right), \text{ and} \tag{8}$$

$$\tau = H^T\Gamma, \tag{9}$$

where $m_r^+ \in \mathbb{R}^{(n-p)\times(n-p)}$ is the internal reduced inertia matrix, $Q_r^+ \in \mathbb{R}^{n-p}$ is the internal reduced force and $\tau \in \mathbb{R}^{n-p}$ is the vector of couplings between antagonist actuation forces (and/or torques). The reader will find, in Boyer and Belkhiri (2014): an recursive algorithm to compute (7)-(9), knowing the kinematic of the tree-like structure, the constraints, its mass geometry and the external forces acting on it; as well as numerical diagrams to solve (6).

4. APPLICATION TO THE HINGE.

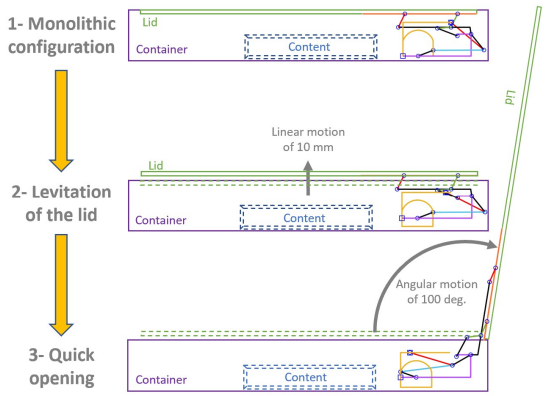

Fig. 3. Opening sequence of the PA.COTTE's luxury product.

Since 2015, the PA.COTTE company has been working on an original IoT product dedicated to the luxury market based on the harmonious wedding of the micro-mechanics and the Cloud technologies. As shown in Fig. 3, the product consists of a container and a lid which protect a valuable content from shocks and fraudulent acts. To make the use "magical", the lid is linked to the container by two actuated hinges (controlled at the owner's request through various on-board or mobile interfaces) which must perform an "impressive" kinematic sequence of opening (or closing). Basically, see Fig. 3, 1) at the rest, the product has a monolithic aspect, that means the lid is fully integrated in the container and the junctures between them are not visible to the user; 2) after an owner's request, the lid performs a vertical linear movement to come out of the container and finally to levitate immobile at few millimeters above it; 3) then, after a short idle delay, the lid performs a fast angular motion from the horizontal to almost 100 deg of tilt. to allow the access of the content to its owner. To achieve this sequence, the PA.COTTE's engineers designed an innovative hinge, which, today, is patented, see Hugues (2020). For space and weight requirements, each hinge is composed by a linear actuator (i.e the assembling of a ball screw, a gearhead and a DC motor) acting on a complex mechanism designed to perform according a continuous action (without change of direction in its motion) of the actuator the two motions of the lid as described above.

4.1 The hinge mechanism.

As defined in Fig. 4, the hinge consists of a non-Grashof 4-bar reverse mechanism composed by a frame $\mathcal{B}_5$ freed vertically in its motion, two rods $\mathcal{B}_3$ and $\mathcal{B}_6$ and an arm $\mathcal{B}_4$ which is connected to the lid $\mathcal{B}_9$. As far as the actuator is concerned, to open the lid, it pulls through the rod $\mathcal{B}_2$ the joint between $\mathcal{B}_3$ and $\mathcal{B}_4$ and pushes it to close the product. Let us note that, at the opening or the closing, $\mathcal{B}_5$ and $\mathcal{B}_6$ have oscillating motions, for whose, at the design stage, the mechanism has been sized so that their motions do not cross singularities and they do not turn backs. To perform the opening sequence describing below, at the 4-bar mechanism has been added a cam and follower mechanism. The idea behind it, is to force one tip of the rod $\mathcal{B}_6$ to follow a specific trajectory. The cam and follower mechanism consists in a cam machined on $\mathcal{B}_0$, three rollers whose one rolls on the inner side of the cam and the two other roll on the outer side, as well as a roller holding connected to the rod $\mathcal{B}_6$, see Fig. 4. According to the geometric design of the cam, it is possible to perform any kind of motion at $\mathcal{B}_6$ and in particular this one that we want.

4.2 Definition of the hinge.

The hinge is a tree-like planar structure of $n+1 = 11$ rigid bodies. Regarding its geometric model, the orientation matrix ${}^iR_j$ and the position vector ${}^iP_j$ of $\mathcal{F}_j$ with respect to $\mathcal{F}_i$ are defined by:

$${}^iR_j = \begin{pmatrix} \cos\theta_j & -\sin\theta_j & 0 \\ \sin\theta_j & \cos\theta_j & 0 \\ 0 & 0 & 1 \end{pmatrix}, \text{ and } {}^iP_j = \begin{pmatrix} x_j \\ y_j \\ 0 \end{pmatrix},$$

where θ_j, x_j and y_j are geometric parameters defined in Tab. 1, whose Fig. 4 gives a schematic view. Moreover, we define by h_o and θ_o, the height and the tilt angle of the lid respectively.

j	$a(j)$	x_j	y_j	θ_j	j	$a(j)$	x_j	y_j	θ_j
1	0	r_1	0	0	6	5	x_{56}	y_{56}	r_6
2	1	0	0	r_2	7	5	x_{57}	y_{57}	r_7
3	2	l_2	0	r_3	8	7	l_7	0	r_8
4	2	l_2	0	r_4	9	8	l_8	0	r_9
5	4	l_4	0	r_5	10	9	l_9	0	r_{10}

Table 1. The geometric parameters.

As far as the kinematic constraints are concerned, there are 9 independent holonomic constraints applied on the hinge reducing the number of degrees of freedom of the mechanism to $n - p = 1$. In the following, we will consider

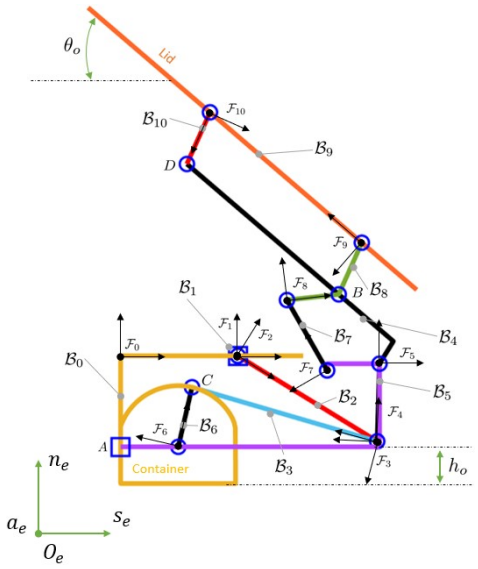

Fig. 4. The tree-like structure of the hinge.

the joint position r_1 as the unique degree of freedom of the hinge. According to Fig. 4, the first eight constraints are:

- two constraints imposed by the prismatic joint between $\mathcal{B}_0$ and $\mathcal{B}_5$ in A:
$$\delta_1^{T0} J_{A_5} = 0, \text{ and } \delta_6^{T0} J_{A_5} = 0;$$
- two constraints imposed by the revolute joint between $\mathcal{B}_4$ and $\mathcal{B}_8$ in B:
$$\delta_1^T ({}^4J_{B_4} - {}^4J_{B_8}) = 0, \text{ and } \delta_2^T ({}^4J_{B_4} - {}^4J_{B_8}) = 0;$$
- two constraints imposed by the revolute joint between $\mathcal{B}_3$ and $\mathcal{B}_6$ in C:
$$\delta_1^T ({}^3J_{C_3} - {}^3J_{C_6}) = 0, \text{ and } \delta_2^T ({}^3J_{C_3} - {}^3J_{C_6}) = 0;$$
- two constraints imposed by the revolute joint between $\mathcal{B}_4$ and $\mathcal{B}_{10}$ in D:
$$\delta_1^T ({}^4J_{D_4} - {}^4J_{D_{10}}) = 0, \text{ and } \delta_2^T ({}^4J_{D_4} - {}^4J_{D_{10}}) = 0.$$

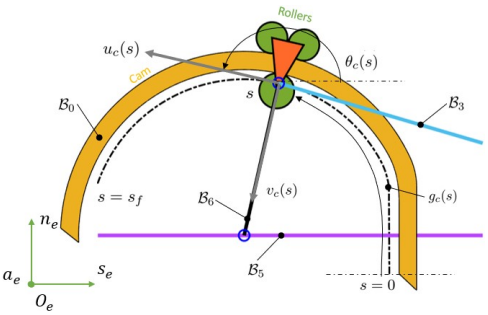

Fig. 5. The cam and the follower mechanism: in yellow, the cam; in green, the rollers (the followers); and, in orange the roller holder.

Regarding the last constraint, it is introduced by the cam and follower mechanism. According to Fig. 5, it is defined as follows:

$$(v_c^T, 0_{1\times 3})^0 J_{C_6} = 0,$$

where v_c is the normal vector at s to the cam curve $g_c : s \in [s_i, s_f] \mapsto g_c(s)$ a C^1 class function, whose their components are equal to: ${}^0v_c = (-\sin\theta_c, \cos\theta_c, 0)^T$, with $\theta_c = \partial g_c/\partial s$. Technically, the curve g_c is composed by three geometric parts which are: A) a segment noted $\mathcal{D}_1$ of length h_1 equivalent to distance travelled by the lid; B) a first arc noted $\mathcal{C}_1$ of radius R_1 to achieve the transition from the linear to angular motions; C) a second arc noted $\mathcal{C}_2$ of radius $R_2 = l_6$ to support the perfect angular motion of the lid. According to this definition, the angle θ_c deriving from g_c, can be easily written analytically with trigonometric functions of the abscissa s and parameters from the design.

Finally, let us remark that, the constraint introduced by the cam being θ_c dependant, the matrix $B \in \mathbb{R}^{9\times 10}$ inherits of this dependency, i.e. $B(r,\theta_c)\dot{r} = 0$. Regarding the kernel $H \in \mathbb{R}^{10\times 1}$, it is also θ_c dependant, which means that, according to (5):

$$\dot{r} = H(r,\theta_c)\dot{r}_1 \text{ , and } \ddot{r} = H(r,\theta_c)\ddot{r}_1 + \dot{H}(\dot{r},\dot{\theta}_c,r,\theta_c)\dot{r}_1,$$

where $\dot{H} \in \mathbb{R}^{10\times 1}$ is function of the temporal derivative of θ_c, i.e. $\dot{\theta}_c$ which, by applying the chain rule, is equal to:

$$\dot{\theta}_c = \frac{\partial\theta_c}{\partial s}\frac{\partial s}{\partial t}, \text{ with } \frac{\partial s}{\partial t} = (u_c^T, 0_{1\times 3})^0 J_{C_6} H \dot{r}_1.$$

4.3 Forward dynamic models of the hinge

According to the definition done at Sec. 4.1 of the hinge, and the general case defined in Sec. 3, the forward dynamic problem under consideration consists in computing at any time the reduced state $x_r : t \in [t_i, t_f] \mapsto x_r^T(t) = (\dot{r}_1, r^T)^T$. Nevertheless, as mentioned at the end of the last section, H and $\dot{H}$ being θ_c dependant, therefore the reduced dynamics are also. The consequence of this is that we need to add to the state vector x_r, the position of the rollers on the cam, i.e the coordinate s. Thus, the forward dynamic problem will consist to compute $x_r : t \in [t_i, t_f] \mapsto x_r^T(t) = (\dot{r}_1, r^T, s)^T \in \mathbb{R}^{12}$, in solving:

$$\frac{\partial}{\partial t}\begin{pmatrix}\dot{r}_1\\ r\\ s\end{pmatrix} = \begin{pmatrix}-(m_r^+)^{-1}(Q_r^+ - F_1)\\ H\dot{r}_1\\ (u_c^T, 0_{1\times 3})^0 J_{C_6} H \dot{r}_1\end{pmatrix}, \tag{10}$$

knowing the initial state $x_r(t_i)$ and the time evolution of the actuation force F_1 (i.e. the unique non-zero component of the actuation vector Γ). In (10), m_r^+ and Q_r^+ are computed by (7) and (8) for which m^+ and Q^+ are obtained symbolically from the recursive algorithm of Boyer and Belkhiri (2014) taking into account that the mass of all the bodies are negligible except for the lid $\mathcal{B}_9$ which has a weight m_o and a l_o length.

5. THE CONTROL LAW

As far as the control is concerned, in order to have the best accuracy during the fast lid motions, the computed torque method has been choice, in particular, its form in the task space, as introduced in Khalil and Dombre (2002). Let us consider an opening sequence. In that respect, for $t \in [t_i, t_i + T_t + T_b]$, with T_t and T_b the translation and idle periods respectively, the control law of the levitation motion, from the rest to the target h_1 altitude, is defined by:

$$F_1 = m_r^+ (J_{hr}^{-1}(W_{h_o} - \dot{J}_{hr}\dot{r}_1)) + Q_r^+, \tag{11}$$

where $J_{hr} = \delta_2^T J_4 H$ is a Jacobian matrix defining $\dot{h}_o$ as a function of $\dot{r}_1$, and W_{h_o} is the input control vector. From Khalil and Chevallereau (1987), W_{h_o} can take the following PD form, i.e:

$$W_{h_o} = h_1 \ddot{f}_s(t, t_i, t_i + T_t) + K_d(h_1 \dot{f}_s(t, t_i, t_i + T_t) - J_{hr}\dot{r}_1) + K_p(h_1 f_s(t, t_i, t_i + T_t) - \mathrm{dgm}_{h_o}(r_1)), \quad (12)$$

where dgm_{h_o} is the direct geometric model providing the lid altitude h_o as a function of r_1, $f_s : t \in [0, +\infty[\mapsto f_s(t, t_a, t_b)$ is a smooth slope function of C^2 class increasing from 0 to 1 in $[t_a, t_b]$ range, while K_p and K_d are the proportional and derivative gains respectively. Regarding the fast opening of T_r period, i.e for $t \in [t_i + T_t + T_b, t_f]$ (with $t_f = t_i + T_t + T_b + T_r$), the control low is defined as follows:

$$F_1 = m_r^+ (J_{\theta r}^{-1}(W_{\theta_o} - \dot{J}_{\theta r}\dot{r}_1)) + Q_r^+, \quad (13)$$

where $J_{\theta r} = \delta_6^T J_4 H$ is a Jacobian matrix defining $\dot{\theta}_o$ as a function of $\dot{r}_1$, and W_{θ_o} is the input control vector which is equal to:

$$W_{\theta_o} = \theta_o^* \ddot{f}_s(t, t_i + T_t + T_b, t_f) + K_d(\theta_o^* \dot{f}_s(t, t_i + T_t + T_b, t_f) - J_{\theta r}\dot{r}_1) + K_p(\theta_o^* f_s(t, t_i + T_t + T_b, t_f) - \mathrm{dgm}_{\theta_o}(r_1)), \quad (14)$$

where dgm_{θ_o} is the direct geometric model providing the lid tilt θ_o as a function of r_1.

6. RESULTS AND DISCUSSIONS

Let us focus on some relevant numerical and experimental results. Today, as the product of PA.COTTE is still confidential, the authors have voluntary hidden the values of the design parameters of the hinge to the reader.

6.1 The geometric and kinematic models

For this first example, we chose to compute the direct geometric models of the hinge, i.e $h_o = \mathrm{dgm}_{h_o}(r_1)$ and $\theta_o = \mathrm{dgm}_{\theta_o}(r_1)$ as introduced in (12) and (14) respectively. In Fig. 6, we plotted the two functions. We observe that,

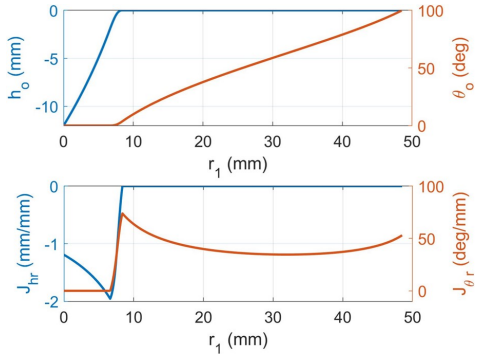

Fig. 6. On top, the direct geometric models dgm_{h_o} and dgm_{θ_o}; on bottom the kinematic models J_{hr} and $J_{\theta r}$.

in the both cases where 1) the hinge performs its linear motion; or 2) its perfect rotational motion; the geometric models can be described analyticity by simple trigonometric expressions. In fact, in the first case, the hinge can be assimilate to a double slider mechanism, while, in the second case, to a slider-crank mechanism, both well documented today. Nevertheless, at the transition between this both kinematic configurations, since the hinge moves and rotates in the same time, no obvious similarity with a known mechanism is likely, thus analytic models are not easy to find and write. For this reason, in the product, numerical forms like look-up tables of these geometric models are used. As far as the kinematic models are concerned, in contrast to the geometric ones, $\dot{h}_o = J_{hr}\dot{r}_1$ and $\dot{\theta}_o = J_{\theta r}\dot{r}_1$ (see Sec. 5) can be analytically calculated knowing Jacobian matrix J_4 and the kernel H. Fig. 6 shows their evolutions according to r_1.

6.2 Integration and hinge control

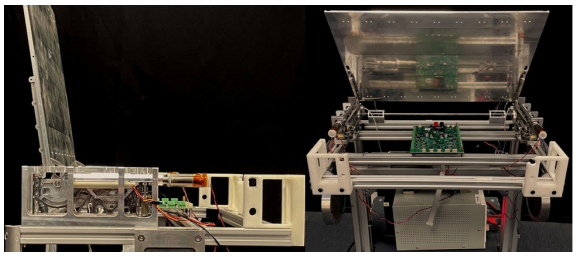

Fig. 7. The experimental mock-up of the opening system. From the left to the right: A side view with the lid fully open; a front view with the lid at 60 deg.

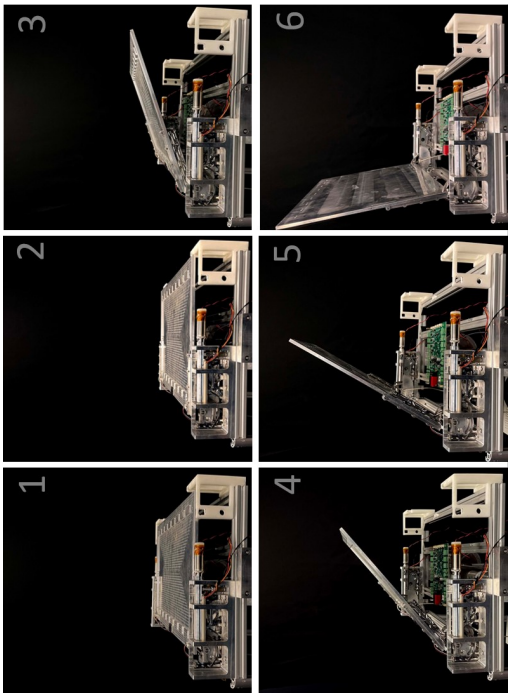

Fig. 8. Snapshots of an opening sequence: 1) the rest; 2) the levitation; 3) opening at 30 deg; 4) opening at 45 deg; 5) opening at 60 deg; 6) lid fully opened.

As a final illustration, let's look at the embedded controller and its integration into an experimental mock-up as shown in Fig. 7. The mock-up is a replica of the PA.COTTE's product, where we find a rigid frame playing the role of the container, two hinges placed on both sides of a plate whose size, weight and rigidity are equivalent of the real lid. The hinge actuators are driven by a common microcontroller. Moreover, mock-up is bound to Matlab/Simulink for the integration, the update, and the on-line monitoring. We have integrated in the mock-up the controllers described

in Sec. 5 at which, in series, we added PI controllers named "current loop" to achieve the regulation with respect to the desired actuation force F_1 the currents crossing the actuators. Finally, as far as the frequencies of the control loops are concerned, the common microncontroller computes at 400 Hz and 2000 Hz the main control loop and the two current loops respectively. Once the computed torque algorithm was implemented in the mock-up, for opening and closing sequences, we recorded r_1 and F_1 (off-line computed through the currents of DC motors) in function of time in order to evaluate the performances of the integrated solution. Fig. 8 shows some snapshots of an opening sequence from the rest to the complete opening of the lid for $T_t = 1$ s, $T_b = 1$ s and $T_r = 1.5$ s while $m_o = 1.2$ kg and $l_o = 230$ mm. In Fig. 10, the real actuation force F_1 as well as $F_{1m} = m_r^+ J_{\theta r}^{-1}(\ddot{\theta}_o^* \ddot{f}_s - \dot{J}_{\theta r}\dot{r}_1) + Q_r^+$ the component coming from the dynamic model and F_{1c} that coming from the PD part of (13) are given. We observe a good estimation of the dynamic behaviour of the hinge. Regarding the trajectory, the tilt error is inferior of 6 percent. Finally, Fig. 10 shows a recording of the actuation force as well as the trajectory for a closing sequence of the lid. As previously, the force estimation and the path following are good and acceptable according the requirements.

7. CONCLUSIONS

In this paper, we have presented an application of a modelling methodology dedicated to the multibody system with closed loops. Based on Newton-Euler approach of robots dynamics Khalil and Dombre (2002) as well as the reduction process of Boyer and Belkhiri (2014), the strategy is successfully applied to the modelling and dynamic control of the hinge of a luxury product. In particular, the methodology employed allowed us to model a complex mechanism based on the fusion of a 4-bar reverse mechanism with a cam and follower mechanism without geometric and kinematic tricks. In our future work, we plan to improve the model by investigating the friction (see Liu et al. (2015)), by making a parameter identification, and so on ... in order to integrate, soon, haptic control functions, like hand detection, manipulation assistance, etc ... i.e many useful and magical new features for the PA.COTTE's products!

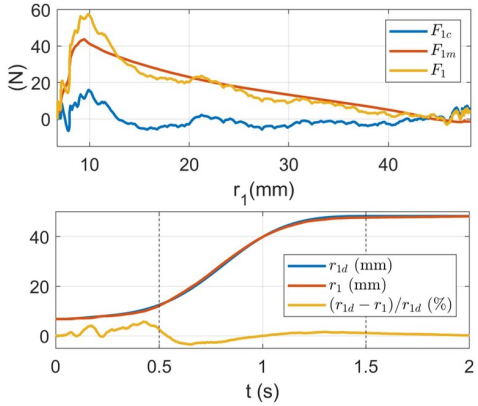

Fig. 9. For an opening angular motion, on top, F_1 in function of r_1; on bottom, the joint trajectory.

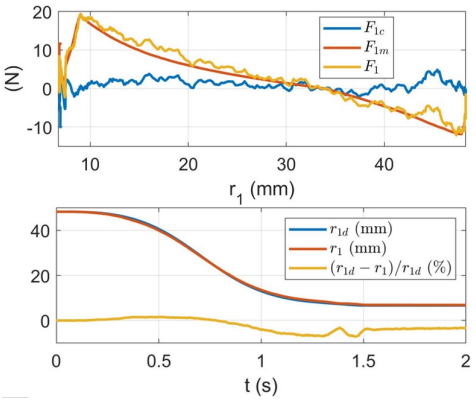

Fig. 10. For a closing angular motion, on top, F_1 in function of r_1; on bottom, the joint trajectory.

REFERENCES

Boyer, F. and Porez, M. (2015). Multibody system dynamics for bio-inspired locomotion: from geometric structures to computational aspects. *Bioinspiration & Biomimetics*, 10(2), 025007.

Boyer, F., Porez, M., and Mauny, J. (2018). reduced dynamics of the non-holonomic whipple bicycle. *Journal of Nonlinear Science*, 28(3), 943–983.

Boyer, F. and Belkhiri, A. (2014). Reduced locomotion dynamics with passive internal DoFs: Application to nonholonomic and soft robotics. *IEEE Transactions on Robotics*, 30(3), 578–592.

Featherstone, R. (2008). *Rigid Body Dynamics Algorithms*. Springer.

Fisette, P., Peťerkenne, J., Vaneghel, B., and Samin, J. (2000). A multibody loop constraints approach for modelling cam/follower devices. *Nonlinear Dynamics*, 22, 335–359.

Fisette, P. and Samin, J. (1994). A new wheel/rail contact model for independent wheels. *Archive of Applied Mechanics*, 64, 180–191.

Hugues, P. (2020). Mechanism for opening/closing an opening leaf with respect to a frame. US patent US2020367626.

Khalil, W. and Chevallereau, C. (1987). An efficient algorithm for the dynamic control of robots in the cartesian space. In *In Proc. IEEE Conference on Decision and Control*, 582–588. Los Angeles, USA.

Khalil, W. and Dombre, E. (2002). *Modeling, Identification and Control of Robots*. Hermes Penton Ltd.

Khalil, W., Gallot, G., and Boyer, F. (2007). Dynamic modeling and simulation of a 3-D serial eel-like robot. *IEEE Transactions on Systems, Man and Cybernetics, Part C (Applications and Reviews)*, 37(6), 1259–1268.

Liu, Y., Li, J., Zhang, Z., Hu, X., and Zhang, W. (2015). Experimental comparison of five friction models on the same test-bed of the micro stick-slip motion system. *Mechanical Sciences*, 6, 15–28.

Murray, R.M., Li, Z., and Sastry, S.S. (1994). *A mathematical introduction to robotic manipulation*. CRC press.

Porez, M., Boyer, F., and Belkhiri, A. (2014). A hybrid dynamic model for bio-inspired soft robots - application to a flapping-wing micro air vehicle. In *In Proc. IEEE International Conference on Robotics and Automation*, 3556–3563. Hong-Kong, China.